

Effect of Ti, V, Cr, and Mn additions on the magnetic properties of a nanocrystalline soft magnetic Fe-Zr-B alloy with high magnetic flux density

| | |
|------------------------------|---|
| 著者 | 牧野 彰宏 |
| journal or publication title | Journal of Applied Physics |
| volume | 85 |
| number | 8 |
| page range | 5127-5129 |
| year | 1999 |
| URL | http://hdl.handle.net/10097/47348 |

doi: 10.1063/1.369099

Effect of Ti, V, Cr, and Mn additions on the magnetic properties of a nanocrystalline soft magnetic Fe–Zr–B alloy with high magnetic flux density

T. Bitoh,^{a)} M. Nakazawa, and A. Makino

Central Research Laboratory, Alps Electric Company, Limited, Nagaoka 940-8572, Japan

A. Inoue

Institute for Materials Research, Tohoku University, Sendai 980-8577, Japan

T. Masumoto

The Research Institute of Electrical and Magnetic Materials, Sendai 982-0807, Japan

The effect of the addition of Ti, V, Cr, and Mn on the magnetic properties of a nanocrystalline soft magnetic Fe–Zr–B alloy has been investigated. The addition of the elements increases both the crystallization temperature and the grain size of α -Fe. After crystallization, these elements are observed in both the α -Fe grains and the residual amorphous matrix. It has been found that V is a useful element to control magnetostriction by keeping the saturation magnetic flux density (B_s) high. The simultaneous addition of V and Mn increases B_s . The alloys with high B_s , above 1.75 T, show good soft magnetic properties as well; the Fe₉₀V₁Zr₆B₃ alloy exhibits high B_s of 1.75 T and high permeability (μ_e) of 31 000, and the Fe_{89.5}V_{0.5}Mn₁Zr₆B₃ alloy exhibits high B_s of 1.78 T and high μ_e of 23 000. These high B_s values are almost the same as that of a Fe-6.5 wt % Si alloy. The alloys also exhibit low core loss. Therefore, nanocrystalline Fe–V–(Mn)–Zr–B alloys are expected to be applied to power electronic devices such as power transformers. © 1999 American Institute of Physics. [S0021-8979(99)37308-4]

I. INTRODUCTION

Recently nanocrystalline soft magnetic alloys consisting of body-centered-cubic (bcc) nanoscale crystallites embedded in a residual amorphous minority matrix have been obtained by crystallizing melt-spun amorphous ribbons.^{1–4} In particular, nanocrystalline Fe-rich Fe–M–B (M=Zr, Hf, Nb) alloys are attractive because these alloys exhibit a high saturation magnetic flux density (B_s) from 1.5 to 1.7 T as well as good soft magnetic properties.

The soft magnetic properties of nanocrystalline Fe–M–B alloys can be improved by the addition of elements. We have already reported the effect of the addition of elements (e.g., Pd, Cu, and Co) on the structure and the soft magnetic properties of nanocrystalline soft magnetic Fe–M–B alloys. The addition of these elements improves the soft magnetic properties. The Pd or Cu addition decreases the α -Fe grain size.^{5,6} On the other hand, the addition of Co to Fe–Zr–B alloys with negative magnetostriction (λ_s) achieves zero λ_s .⁷ In this article, the effect of the addition of Ti, V, Cr, and Mn on the magnetic properties of a nanocrystalline soft magnetic Fe–Zr–B alloy are presented.

II. EXPERIMENTAL PROCEDURE

Fe–TM–Zr–B (TM=Ti, V, Cr, Mn) alloy ingots were prepared by arc melting in an Ar atmosphere. The rapidly solidified ribbons, 15 mm in width and 20 μ m in thickness, were produced by a single-roller melt-spinning method in an Ar atmosphere. The annealing treatment of the as-quenched

samples was carried out by keeping the samples at 903 K for 300 s in a vacuum at a heating rate of 3 K/s.

The saturation magnetic flux density (B_s) under an applied field of 800 kA/m and the coercivity (H_c) under a maximum applied field of 800 A/m were measured with a vibrating sample magnetometer (VSM) and a low frequency B – H loop tracer, respectively. The permeability (μ_e) at 1 kHz under an applied field of 0.4 A/m and the core loss (W) at 50 Hz were measured with a vector impedance analyzer and an ac B – H loop analyzer, respectively. The saturation magnetostriction (λ_s) under an applied field of 40 kA/m was measured by a strain gauge technique. The crystallization temperature (T_x) of the amorphous alloys was determined by differential thermal analysis (DTA) at a heating rate of 0.17 K/s. The mean size (D) was evaluated from the half-width of the α -Fe (110) x-ray diffraction peak. The microstructure was observed by a transmission electron microscopy (TEM).

III. RESULTS AND DISCUSSION

First, we examined the microstructure of the nanocrystalline Fe_{86.5}TM_{3.5}Zr₇B₃ (TM=Ti, V, Cr, Mn) alloys by high-resolution TEM (HRTEM). Figure 1(a) shows the HRTEM image of the crystallized Fe_{86.5}V_{3.5}Zr₇B₃ alloy. The alloy consists of nanoscale α -Fe grains, 10–20 nm in size, embedded in a residual amorphous matrix. The composition of the α -Fe grains and the residual amorphous matrix were examined by energy-dispersive spectroscopy (EDS) analysis using an electron beam with a diameter of 1 nm. Figure 1(b) shows the result for the α -Fe grain and Fig. 1(c) shows the result for the residual amorphous matrix. As already reported, the residual amorphous matrix is enriched by Zr.^{3,4}

^{a)}Electronic mail: bitohter@alps.co.jp

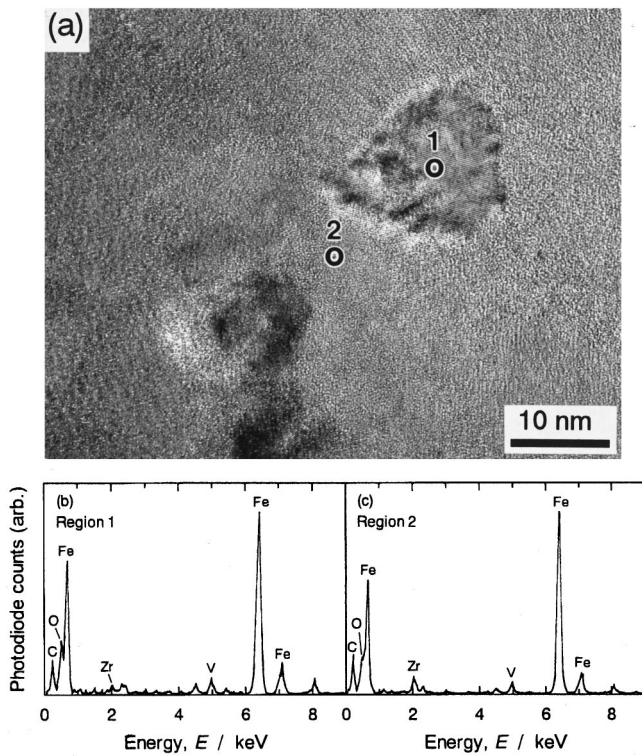


FIG. 1. (a) HRTEM image and EDS spectra taken from (b) the α -Fe grains (region 1) and (c) the residual amorphous matrix (region 2) of the nanocrystalline $\text{Fe}_{86.5}\text{V}_{3.5}\text{Zr}_7\text{B}_3$ alloy.

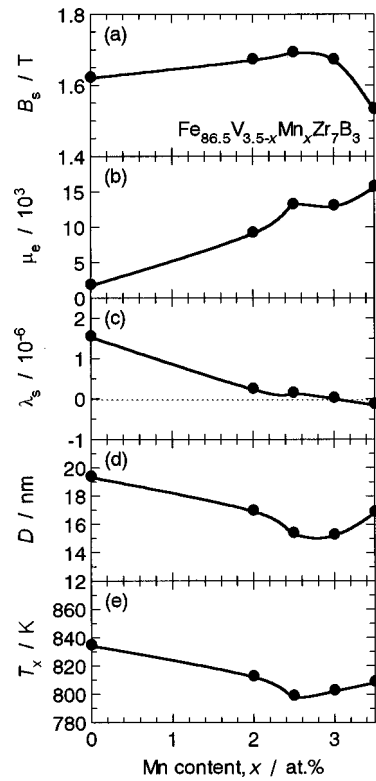


FIG. 3. Changes in (a) the saturation magnetic flux density (B_s), (b) the permeability (μ_e), (c) the magnetostriction (λ_s), (d) the mean grain size (D), and (e) the crystallization temperature (T_x) as functions of the Mn content (x) of the nanocrystalline $\text{Fe}_{86.5}\text{V}_{3.5-x}\text{Mn}_x\text{Zr}_7\text{B}_3$ alloys.

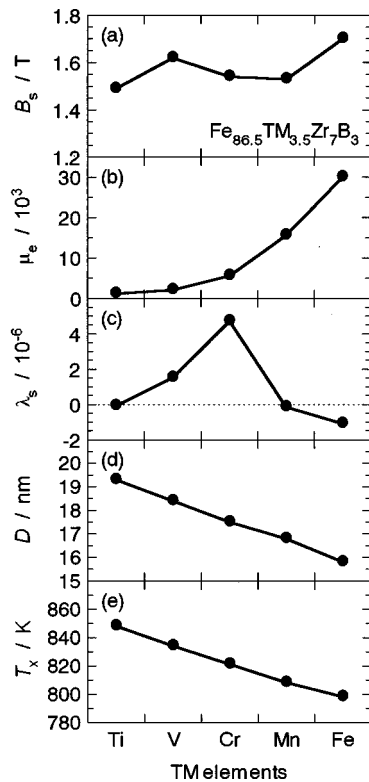


FIG. 2. TM element dependence of (a) the saturation magnetic flux density (B_s), (b) the permeability (μ_e), (c) the magnetostriction (λ_s), (d) the mean grain size (D), and (e) the crystallization temperature (T_x) of the nanocrystalline $\text{Fe}_{86.5}\text{TM}_{3.5}\text{Zr}_7\text{B}_3$ (TM=Ti, V, Cr, Mn) alloys.

There is V in both the α -Fe grains and the residual amorphous matrix. The microstructure observed for $\text{Fe}_{86.5}\text{TM}_{3.5}\text{Zr}_7\text{B}_3$ (TM=Ti, Cr, Mn) alloys was similar.

Figure 2 shows the saturation magnetic flux density (B_s), the permeability (μ_e), the magnetostriction (λ_s), the mean grain size (D), and the crystallization temperature (T_x) of the nanocrystalline $\text{Fe}_{86.5}\text{TM}_{3.5}\text{Zr}_7\text{B}_3$ (TM=Ti, V, Cr, Mn) alloys. The addition of TM elements decreases both B_s and μ_e . The crystallization temperature (T_x) is increased by

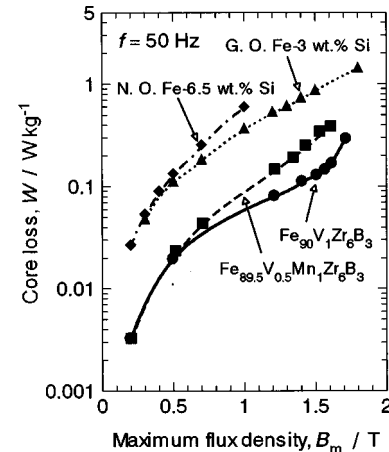


FIG. 4. Changes in the core loss (W) as a function of the maximum flux density (B_m) for the nanocrystalline $\text{Fe}_{90}\text{V}_1\text{Zr}_6\text{B}_3$ and $\text{Fe}_{89.5}\text{V}_{0.5}\text{Mn}_1\text{Zr}_6\text{B}_3$ alloys, the grain-oriented (G. O.) Fe-3 wt % Si alloy, and the nonoriented (N. O.) Fe-6.5 wt % Si alloy.

TABLE I. Saturation magnetic flux density (B_s), permeability (μ_e), coercivity (H_c), magnetostriction (λ_s), and core loss (W) of the nanocrystalline $\text{Fe}_{90}\text{Zr}_7\text{B}_3$, $\text{Fe}_{91}\text{Zr}_6\text{B}_3$, $\text{Fe}_{90}\text{V}_1\text{Zr}_6\text{B}_3$ and $\text{Fe}_{89.5}\text{V}_{0.5}\text{Mn}_1\text{Zr}_6\text{B}_3$ alloys.

| | B_s (T) | μ_e^a | H_c (A/m) | λ_s (10^{-6}) | W^b (W/kg) |
|--|--------------|-----------|----------------|------------------------------|-----------------|
| $\text{Fe}_{90}\text{Zr}_7\text{B}_3$ | 1.70 | 30 000 | 5.8 | -1.1 | 0.21 |
| $\text{Fe}_{91}\text{Zr}_6\text{B}_3$ | 1.77 | 16 000 | 19.2 | -1.3 | 0.40 |
| $\text{Fe}_{90}\text{V}_1\text{Zr}_6\text{B}_3$ | 1.75 | 31 000 | 4.6 | -0.3 | 0.11 |
| $\text{Fe}_{89.5}\text{V}_{0.5}\text{Mn}_1\text{Zr}_6\text{B}_3$ | 1.78 | 23 000 | 9.1 | -0.9 | 0.21 |

^a0.4 A/m, 1 kHz.

^b1.4 T, 50 Hz.

the addition of the TM elements. This behavior is similar to that observed in $\text{Fe}_{80-x}\text{TM}_x\text{P}_{13}\text{C}_7$ amorphous alloys.⁸ It should be noted that D is strongly related to T_x ; the grain size increases as T_x becomes higher.

The addition of TM elements changes λ_s of the alloy to the positive side. This behavior can be explained by the change of λ_s for the α -Fe grains.⁹ Since the $\text{Fe}_{90}\text{Zr}_7\text{B}_3$ alloy has negative λ_s of -1.1×10^{-6} , it is expected that zero λ_s can be obtained by the addition of TM elements. The number of additives required to obtain zero λ_s is smallest for Cr and increases in the order of $\text{V} < \text{Ti} \approx \text{Mn}$. As shown in Fig. 2(a), the addition of these elements decreases B_s . However, the V containing alloy exhibits higher B_s (1.62 T) than that of the other alloys (1.49–1.54 T). It has been reported that bulk Fe–V alloys exhibit a higher Curie temperature (T_c) than that of pure α -Fe.¹⁰ The high T_c is favorable for obtaining high B_s at room temperature. Therefore, V is a useful element for controlling λ_s while keeping B_s high.

However, the $\text{Fe}_{86.5}\text{V}_{3.5}\text{Zr}_7\text{B}_3$ alloy exhibits a low μ_e of 2000. In order to obtain a high μ_e as well as a high B_s , we examined the possibility of simultaneous additions of V and Mn because the $\text{Fe}_{86.5}\text{Mn}_{3.5}\text{Zr}_7\text{B}_3$ alloy exhibits a high μ_e of 16 000. Figure 3 shows changes in B_s , μ_e , λ_s , D , and T_x as functions of the Mn content (x) of the nanocrystalline

$\text{Fe}_{86.5}\text{V}_{3.5-x}\text{Mn}_x\text{Zr}_7\text{B}_3$ alloys. The high permeability (μ_e) above 10 000 was obtained with $x \geq 2$. It should be noted that the simultaneous addition of V and Mn increases B_s . The $\text{Fe}_{86.5}\text{V}_1\text{Mn}_{2.5}\text{Zr}_7\text{B}_3$ alloy shows high B_s of 1.69 T, high μ_e of 13 000, and nearly zero λ_s simultaneously. This alloy also has the lowest T_x of 798 K and the small D of 15 nm.

Finally, we examine the addition of V or the simultaneous addition of V and Mn in improving the soft magnetic properties of the $\text{Fe}_{91}\text{Zr}_6\text{B}_3$ alloy. As shown in Table I, the $\text{Fe}_{91}\text{Zr}_6\text{B}_3$ alloy exhibits high B_s of 1.77 T and μ_e of 16 000. The $\text{Fe}_{90}\text{V}_1\text{Zr}_6\text{B}_3$ alloy exhibits high B_s of 1.75 T, high μ_e of 31 000, and sufficiently small λ_s of -0.3×10^{-6} . The addition of V reduces the magnitude of λ_s and improves the soft magnetic properties by keeping B_s high. The $\text{Fe}_{89.5}\text{V}_{0.5}\text{Mn}_1\text{Zr}_6\text{B}_3$ alloy exhibits high B_s of 1.78 T and high μ_e of 23 000. These high B_s values are almost the same as that of the Fe-6.5 wt % Si alloy. Figure 4 shows the core loss of the $\text{Fe}_{90}\text{V}_1\text{Zr}_6\text{B}_3$ and $\text{Fe}_{89.5}\text{V}_{0.5}\text{Mn}_1\text{Zr}_6\text{B}_3$ alloys, the grain-oriented Fe-3 wt % Si alloy, and the nonoriented Fe-6.5 wt % Si alloy. The nanocrystalline Fe–V–Zr–B and Fe–V–Mn–Zr–B alloys exhibit lower core loss than the Fe–Si alloys. Therefore, these nanocrystalline alloys are expected to be applied to power electronic devices such as power transformers because of their high B_s and low core loss.

¹Y. Yoshizawa, S. Oguma, and K. Yamauchi, *J. Appl. Phys.* **64**, 6044 (1988).

²G. Herzer, *Mater. Sci. Eng., A* **133**, 1 (1991).

³A. Makino, K. Suzuki, A. Inoue, and Y. Hirotsu, *J. Magn. Mater.* **133**, 329 (1994).

⁴A. Makino, A. Inoue, and T. Masumoto, *Mater. Trans., JIM* **36**, 924 (1995).

⁵A. Makino, A. Inoue, and T. Masumoto, *Nanostruct. Mater.* **6**, 985 (1995).

⁶A. Makino, T. Bitoh, A. Inoue, and T. Masumoto, *J. Appl. Phys.* **81**, 2736 (1997).

⁷K. Suzuki, A. Makino, A. Inoue, and T. Masumoto, *J. Phys. Soc. Jpn.* **18**, 800 (1994).

⁸M. Naka, S. Tomizawa, T. Watanabe, and T. Masumoto, *Proceedings of the 2nd International Conference on Rapidly Quenched Metals* (MIT Press, Cambridge, 1975), p. 273.

⁹R. C. Hall, *J. Appl. Phys.* **31**, 1937 (1960).

¹⁰H. Asano, *J. Phys. Soc. Jpn.* **27**, 524 (1969).